

Hyperthermia by Near Infrared Radiation Induced Immune Cells Activation and Infiltration in Breast Tumor

Wan Fatin Amira Wan Mohd Zawawi

Universiti Teknologi Malaysia

Merilyn Hibma

University of Otago

Maheza Ima Salim

Universiti Teknologi Malaysia

Khairunadwa Jemon (✉ khairun_nadwa@utm.my)

Department of Biosciences, Faculty of Science, Universiti Teknologi Malaysia, 81310, Johor, Malaysia

Research Article

Keywords: Breast cancer, Immunohistochemical analysis, favourable anti-tumor immune response

Posted Date: January 7th, 2021

DOI: <https://doi.org/10.21203/rs.3.rs-125646/v1>

License:  This work is licensed under a Creative Commons Attribution 4.0 International License. [Read Full License](#)

Abstract

Breast cancer is the most common cancer that causes death in women. Conventional therapies, including surgery and chemotherapy, have different therapeutic effects and are commonly associated with risks and side effects. Near infrared radiation is a technique with few side effects that is used for local hyperthermia, typically as an adjuvant to other cancer therapies. The understanding of the use of near NIR as a monotherapy, and its effects on the anti-tumour immune response, is limited. In this study we investigate the effects of HT treatment using NIR on tumor regression and on the anti-tumor immune response in breast tumors. Results demonstrated that local HT by NIR at 43°C reduced tumor progression and prolonged the survival of tumor-bearing mice. Immunohistochemical analysis revealed a significant reduction in proliferation in treated tumor, which was accompanied by an abundance of heat shock protein 70 (Hsp70). Increased numbers of activated dendritic cells were observed in the draining lymph nodes of the mice, along with infiltration of T cells, NK cells and B cells into the tumor. In contrast, tumor-infiltrated regulatory T cells were largely diminished from the tumor. In addition, higher IFN- γ and lower IL-10 secretion was observed in blood of treated mice. Overall, this present study extends the understanding of using local HT by NIR to stimulate a favourable anti-tumor immune response against breast cancer.

Introduction

Breast cancer is the most common cancer among women, regardless race or ethnicity. The number of new cases increases each year with the growing of population. A variety of treatments that are available, however almost all conventional treatments, including chemotherapy and surgery, come with side effects. Hyperthermia (HT) which one of many cancer treatments available, is a therapy that uses heat to increase body temperature above the normal temperature. This could be achieved either systemically, or locally at a particular area of the body. As a non-invasive cancer treatment strategy, local HT is ideally suitable to treat superficial tumors such as neck or breast tumors ^{1,2}, where the temperature given is readily attainable and tolerable to patients ^{3,4}. Local HT can be either within the range of 39-48°C or exceed temperature around 70-90°C, at which different temperature could give different effects to the tumor and the adjacent normal tissues ^{5,6}. The main objective of local moderate HT is to kill, weaken, or sensitise the cancer cells ⁷ as well as to improve the anti-tumor immunity ⁸, without affecting the surrounding normal tissues ⁹.

Besides inhibiting tumor growth by necrosis and apoptosis ^{10,11}, multiple cancer-related studies have reported the application of fever-range HT as an immunotherapeutic agent ¹². HT was reported to stimulate the activation of antigen presenting cells (APCs) by releasing the heat shock protein (Hsp) from the dying heat-stressed cancer cells ¹³. In addition, these dying cells also produce exosomes that assist the maturation of APCs and increasing tumour-specific cytotoxic T lymphocyte (CTL) response ^{14,15}. High level of lymphocytes was also observed in lymph node of mice treated with HT, implying the augmentation of immune response by HT treatment ¹². Local HT applied at 40-43°C also facilitates immune cells trafficking towards tumor by increasing the permeability of tumor vasculature and perfusion ⁶. Furthermore, electro-HT provides favourable tumor microenvironment (TME) for immune cells to function optimally, hence would be beneficial for combination with immunotherapy ^{16,17}.

Despite showing some clinical benefits, HT still can be regarded as an uncommon therapy for cancer in clinical practice. This could be partly due to the inadequate monitoring of the thermal dose or tumor temperature during the treatment ¹⁸. Furthermore, a safe and effective treatment protocol is very crucial for HT to be a candidate in clinical application. The use of near infrared radiation (NIR), one of the many approaches for local HT treatment, has been attractive to researchers and physicians. Unlike conventional radiation therapy, this technique omits the use of high energy radiation that could severely damage the normal cells ¹⁹, thus resulting in a better outcome in cancer treatment. In fact, the irradiation is selective to cancerous tissue while avoiding the suppression of host immune response, thus enabling the host to achieve a maximum immune response ²⁰. However, NIR is primarily used in photothermal and photodynamic therapy which require the assistance from nanoparticles and photosensitizer ²¹. Additionally, NIR has always been used as an adjuvant to other therapy including immunotherapy ^{22,23}. To best of our knowledge, there are limited numbers of studies to date reporting the anti-tumor response in breast tumors following monotherapy of NIR as a heat source, thus our study aimed to fill this gap.

This study was undertaken to confirm and extend the understanding of using local HT by NIR as a heat source in generating anti-tumor immunity. In the present paper, using a subcutaneous breast tumor model, we report immune cell activation and infiltration following HT treatment that leads to the enhanced anti-tumor response.

Results

Local HT by NIR reduces tumor growth in tumor-bearing mice

Mice that were injected with EMT6 cells (Fig. 1a) all had palpable sub-cutaneous tumors by day 7 post-injection, ranging from 25 to 40 mm² in size. When the tumors were irradiated at day 7, the tumor reached 43°C in less than 10 min and that temperature was maintained for 30 min thereafter. Figure 1b shows the tumor growth profile in the HT treatment group in comparison with untreated control group. Tumor growth in HT treated mice was delayed by 58% as compared to the tumor growth in control group. However, this data is not significant which may be due to the variation in tumor sizes between individual mice in treated group. As shown in the graph, there were two distinct tumor profile, with one showing a slow increment and the other one showing a reduction in tumor size. Four out of 11 (36%) in the HT treated group were tumor-free within two weeks following the treatment and remained tumor-free for 50 days thereafter before euthanized. This result was accompanied by a significant increase ($P < 0.0001$; Mantel-Cox analysis) in the median survival (19.5 and 26.5 for control and HT treated group, respectively) (Fig. 1c).

Local HT by NIR reduces tumor cells proliferation

To investigate the effect of HT on tumor tissue, tissue was harvested and processed for immunohistochemical analysis 24 h after the last treatment (Fig. 2a). Proliferating cell nuclear antigen (PCNA) is essential for cellular processes such as DNA replication²⁴ and commonly used as a marker of cell proliferation. Immunostaining of tissue section with PCNA demonstrated large numbers of actively proliferating tumor cells in the untreated group at 24 h post-treatment (Fig. 2b). Meanwhile, a reduced proportion of areas with PCNA-positive cells was observed in treated tumor. Although there were some residual cells with proliferating activity at the tumor edge, overall data confirmed the inhibition of proliferation in HT group. In addition, it was observed that the nuclei in treated tumor were larger when compared to untreated tumor, suggesting the heterogeneity across the treated tumor which may consists of other cell types including immune cells. The significant reduction ($P < 0.005$; Student's *t*-test) of cell proliferation in the tumor tissue indicates the retardation of tumor growth. This finding was also in line with our pathological examination of the HT-treated tumor tissue, which showed prominently dead tumor cells, implying necrosis²⁵ and apoptosis²⁶ following HT (results not shown).

Local HT by NIR increases tumor Hsp70 expression

HT has been reported to induce heat stress to the cells. In response to this adverse stress, the expression of heat shock proteins would normally be increased²⁷. We therefore wanted to measure Hsp expression in response to HT treatment. To test this, mice were injected subcutaneously with EMT6 cells, the tumor was irradiated three times at days 7, 8 and 9 post injection, and the tumor tissue was harvested one day later for immunohistochemical staining for Hsp70 (Fig. 3a). In HT-treated group, Hsp70 was strongly expressed and abundantly distributed around the necrotic area that spread along the peripheral region of the tumor (Fig. 3b). In contrast, there was no Hsp70 detected in the untreated tumor.

Local HT by NIR increases DC activation in lymph node and tumor-infiltrated T cells

An early step in initiation of the adaptive anti-tumor immune response is the uptake of tumour antigen by APCs, followed by the presentation to T cells of tumor associated peptides in the major histocompatibility (MHC) I or MHC II complex. As a key player in the adaptive immune response, we evaluated the number of activated CD11c⁺ dendritic cells in dLN at 24 h after the last HT treatment (Fig. 4a). Cells were gated based on forward and side scatter profile to exclude the doublet cells. Lymphocytes were then gated and further analyzed for the presence of CD11c. The activation and maturation of DCs was also determined by measuring the expression of co-stimulatory molecules CD80 and CD86 on the positive CD11c cells. There was a significant increase ($P < 0.005$; Student's *t*-test) in the number of CD11c⁺ cells in the tumor dLN of the HT treated group when compared to the control group (Fig. 4b). In addition, expression of CD86 and CD80 was increased in the HT treated group, compared with the control group, implying higher DCs activation in lymph node following HT by NIR (Fig. 4c).

The infiltration of CD3⁺ T cells in tumor has been used to predict prognosis in cancer and is associated with active recruitment of T cells responsible for cell death^{28,29}. We enumerated the number of CD3⁺ T cells that infiltrated the tumor by staining with an anti-CD3 antibody. Our result from immunohistochemical staining showed a non-significant increase of CD3⁺ T cells in heated tumor, which suggests that T cells have been activated by mature DCs and trafficked into the tumor (Fig. 4d).

Local HT by NIR increases CD8 but not CD4 infiltration into EMT6 breast tumor

To elucidate CD4 helper T cell and CD8 cytotoxic T cell infiltration into the tumor following HT treatment, tumor tissue was harvested at day 14 and 21 post-inoculation and immunohistochemical analysis was carried out (Fig. 5a). Figure 5b shows that HT had little effect on the number of tumor infiltrated CD4⁺ T cells, with only a slight difference observed between both groups. On the other hand, the number of CD8⁺ T cells showed a significant increase on treated tumor at both timepoints, with higher CD8⁺ T cells number was observed at day 21 (Fig. 5c). This result was further validated using flow cytometric analysis (Fig. 6a and Supplementary Fig. S1). As expected, there was significant difference ($P < 0.005$; Student's *t*-test) between both groups, with treated group shows higher percentage of CD3⁺CD8⁺ T cells as compared to control (Fig. 6b).

Local HT by NIR inhibits regulatory T cells infiltration in tumor

We investigated the effect of NIR on the immunosuppressive cells, particularly regulatory T cells (Tregs). Tregs is a sub-population of T cells, described as expressing CD4, CD25, and FoxP3. Tregs infiltrating the tumor was examined at day 21 post-inoculation. Flow cytometric analysis in Fig. 6c shows a low number of CD4 T cells co expressing CD25 and FoxP3 in NIR-treated tumor, at around 80% reduction as compared to control. The percentage of CD4⁺CD25⁺FoxP3⁺ Tregs among the total tumor-infiltrated CD4⁺ cells is 44.45 ± 9.026 in control group compared to 6.468 ± 1.176 in NIR treated group ($P < 0.005$; Student's *t*-test). In light of the notable CD8 T cell infiltrate in the NIR samples, we also calculated the ratio of CD8 to Tregs that had infiltrated the tumor. The median of CD8:CD4⁺CD25⁺FoxP3⁺ Tregs was significantly higher in NIR treated group as compared to control (0.0076 and 0.91 at $P = 0.0286$, respectively). This result is consistent with a good prognosis, as shown by Preston *et al.* (2013), who reported a higher CD8:Treg ratio in ovarian cancers that had a good prognosis. The suppression of immune response by Tregs is often linked to poor naïve T cell proliferation^{30,31}. Therefore, depletion of Tregs shown in this experiment supports the results described in Fig. 6b that show a high number tumor-infiltrated CD8 T cells, confirming the enhancement of CD8 T-cell effector function in eradicating tumor.

Effect of local HT by NIR to intratumoral cytokine

To further understand the effect of NIR on the immune response, we next measured intratumoral cytokines including IFN- γ , TNF- α , IL-2 and IL-10 at 21 days post-inoculation (Fig. 7a). These cytokines were selected as they play a diverse role in breast cancer progression and adaptive immunity. Tumor was measured for total protein concentration and analyzed by Luminex technology for cytokine concentration. Our findings demonstrated a non-significant increase of IFN- γ in tumor of treated mice compared to untreated mice (Fig. 7b). Besides, IL-2 level in HT treated tumor displayed a slight increase, while the concentrations of TNF- α and IL-10 showed no obvious changes as compared to control group.

Discussion

Local HT treatment has been widely used to treat solid tumors in experimental models^{32–34} and in cancer patients^{35–38}. Heat may come from various external sources including infrared radiation, radiofrequency, microwave and ultrasound, where these approaches could give different effects in eradicating the tumor. Potentially, NIR was reported to be efficient in killing the tumor cells selectively without causing disruption on surrounding normal tissues. In this study, heat was applied using WIRA with a 750 watt halogen lamp and a 780 nm high pass filter, resulting a peak output at 820 nm. This device is commonly used to treat skin diseases, wound and many other areas of medicines. WIRA is easy to operate, gentle to skin and allows deeper penetration compared to conventional infrared therapy³⁹. As breast cancer is a superficial tumor, the use of local HT is clinically appropriate and has potential to treat the tumor effectively. While conducting the local HT procedure, it is very important to monitor the tumor temperature precisely because even the slightest temperature change could give a different level of heat-stress to the tumor and stromal cells. The treatment efficacy could also be temperature dependent. For instance, heating tumor at 42°C may improve vasculature permeability thus better immune cells trafficking into the tumor⁶. This scenario however, was not observed at temperature more than 43°C due to hemorrhage⁶. We selected 43°C for our HT approach because this fever to moderate temperature is believed to be immunotherapeutic⁶. The treatment was repeated three times for 30 minutes each to ensure the optimum effect was achieved.

Using this approach, HT was able to inhibit the growth of subcutaneous EMT6 tumor, with 36% of treated mice showing complete tumor regression. These mice also survived for 50 days after the treatment, demonstrating that HT could provide a therapeutic benefit

that prolongs mice survival. HT caused tumor cells to undergo necrosis and apoptosis which affects the cell number and tumor size and subsequently led to inhibition of tumor growth. Consistent with tumor inhibition, HT also decreased cell proliferation, which was observed through the reduction of PCNA expression. Therefore, we reasoned that NIR not only induce cell death but also retarded the division of new cells by arresting the cell cycle. In particular, NIR induces heat stress to the cells. It was reported that the stress response pathway always elicits cell cycle arrest to circumvent the transmission of damaged macromolecules and provides the time for cells to repair themselves, resulting in suppression of cell proliferation⁴⁰. Accordingly, a more pronounced proliferating activity was found in our untreated breast tumor, which correlates with the findings of other clinical studies that demonstrated PCNA is greatly involved in breast cancer initiation and development^{41,42}

Heat shock proteins have been recognized as an important participant in immune system^{27,43}. Hsps are present in normal cells conditions but will be highly expressed under stress condition including heat-stress. Necrotic cancer cells destroyed by HT will release antigenic tumor peptides that includes Hsp into extracellular matrix. These extracellular Hsps then will act as danger signal to activate dendritic cells and subsequently T cells to generate adaptive immune response. The antitumor effect is dominated by Th1 CD4⁺ T lymphocytes. Generally, CD4 T cells perform immunosurveillance and regulate immune system, alongside with Th1 and Th2 cytokines to balance the cell-mediated immunity⁴⁴. Th1 CD4⁺ T lymphocytes secretes Th1 cytokines including IFN- γ , TNF- α , IL-2 which in turn act as marker for Th1 immune response. In response to cancer, CD4 T cells provide help in the priming of tumor-specific CD8 T cells, thus permitting the differentiation and expansion of tumor antigen-specific CTLs⁴⁵. Subsequently, effector CD8 T cells migrate into the tumor and perform their killing activity accordingly. Similarly, we reported a high level of Hsp in the heated tumor (Fig. 8a), accompanied by increased DC activation in dLN of treated mice (Fig. 8b). Our findings also demonstrated a significant increase of tumor infiltrated-CD8 T cells with greater CD8 T cells infiltrates tumor over time (Fig. 8c). This scenario suggests HT treatment likely stays effective for a longer period, which may be related to higher antigen-specific CTLs produced as a result from increased Hsp-peptide complex cross presentation by DCs⁴⁶.

The upregulation of IFN- γ in tumor also supports these findings (Fig. 8d), where IFN- γ is able to inhibit tumor cell proliferation and differentiation⁴⁵. Besides orchestrating the innate immune response, IFN- γ , which is mainly produced by activated T cells and NK cells, also mediates the adaptive anti-tumor response. For instance, IFN- γ increases the expression of MHC, making them more susceptible to immune recognition and destruction by CD8⁺ T cells⁴⁷. Other than IFN- γ , IL-2 also plays a critical role in the induction of the immune response. However, the non-significant increase in IL-2 reported here maybe due to the dual role played by this cytokine. IL-2 is responsible for regulating CD8 effector function as well as promoting the differentiation of CD4⁺ T lymphocytes into Tregs. On another note, these intratumoral cytokines were analyzed 2 weeks post-treatment, which is considerably late as they usually secreted at the early stage to help initiate the immune response. This may also explain the non-significant different in expression between both groups. Hence, future study is suggested to be conducted at day 4–7 post-treatment.

Tregs have long been known to suppress the immune response and favor the growth of tumor cells, causing the cancer to progress and to become metastatic. The recruitment of CD4⁺CD25⁺FoxP3⁺ T cells to the tumor distorts T cells responses from an effector to a regulatory subtype, causing protective antitumor immunity to diminish⁴⁸. As been reviewed by Plitas and Rudensky (2020), the presence of this population in tumor microenvironment is linked with the suppression of T cells, NK cells and DC in animal models and in cancer patients⁴⁹. Similar situations observed in our data correlate with those findings, suggesting the effectiveness of NIR in limiting the immunosuppressive activity (Fig. 8e). The CD8:Treg ratio is commonly used to predict prognosis in breast cancer^{50,51}. NIR also causes higher CD8:Treg ratios at D21 post-inoculation, which implies a favorable prognosis. In conjunction with these results, HT is believed to disrupt the function of Tregs and interfere with their migratory properties⁵². Additionally, heat stress enhances the cytotoxic activity of NK cells against Tregs⁵³, which also explains our result showing that the Tregs population in the tumor is conversely proportional to NK cells. Taken together, these findings reflect the dampening of immunosuppressive activity mediated by HT by NIR.

Collectively, our data suggest that a monotherapy of NIR is able to activate and promote the infiltration of immune cells in breast tumor, thus may be an effective in the treatment of breast cancer. With easy administration in a controlled manner, the application of local hyperthermia could potentially offer clinical benefit for the treatment of breast cancer.

Methods

Cell line

The mammary carcinoma cell line EMT6 (ATCC CRL-2755) was maintained in Waymouth's MB medium (Life Technologies), supplemented with 10% heat inactivated fetal bovine serum (FBS; Life Technologies) and 1% penicillin/streptomycin (100 U/ml penicillin and 100 µg/ml streptomycin, Sigma).

In vivo tumor model

All animal experiments were performed under the approved protocol by the Universiti Kebangsaan Malaysia Animal Ethics Committee (Approval code: UTM/2016/KHAIRUNADWA/28-JAN./729-FEB.-2016-JAN.2019). This study was conducted in accordance with the ARRIVE and relevant guidelines. Female Balb/c mice (8–10 weeks of age) weighing between 18–25 g were purchased from Universiti Kebangsaan Malaysia, Bangi, Malaysia. Mice were anaesthetized by subcutaneous injection of a cocktail of Ketamine/Xylazine/Zoletil (KTX) at dosage of 0.1 ml/25 g body weight. Mice were inoculated with 5×10^5 EMT6 cells in 100 µl phosphate-buffered saline (PBS, pH 7.4) into the right flank subcutaneously.

Local HT treatment

At day 7 post-EMT6 inoculation, tumors of about 30 mm² in size were subjected to local HT treatment by means of infrared radiation using a water-filtered infrared irradiator (wIRA, Hydrosun 750, Germany). A 30-gauge thermocouple was inserted into tumor center to precisely monitor the tumor temperature. For the irradiation, mice were covered by a circular shield, exposing only the tumor site. The tumor was heated to 43°C, and the temperature was maintained by continuous regulation of the heat source that switched on and off intermittently for 30 min, controlled by the inserted thermocouple. This treatment was repeated for three times, every consecutive day. Tumor size was monitored by measuring the tumor using a digital caliper at every alternate day.

Immunohistochemical analysis

Tumors were harvested at day 10, 14 and 21 post-treatment. Tumor tissues were fixed in 10% neutral-buffered formalin and embedded in paraffin for staining. Formalin-fixed paraffin-embedded (FFPE) tissue sections (4 µm) were deparaffinized in xylene followed by rehydration with a series of alcohol washes. For antigen retrieval, tissue sections were heated for 20 min in 10 mM sodium citrate buffer (pH 6.0) or Tris/5% Urea (pH 9.5). Sections were blocked with 5% skim milk in Tris-buffered saline (TBS) and stained with primary antibodies overnight at 4°C. Rabbit anti-mouse PCNA (clone C19, Abcam), mouse anti-mouse Hsp70 (W27, Santa Cruz), rabbit anti-mouse CD3 (SP7, Abcam), rat anti-mouse CD8 (4SM15, eBioscience) and rabbit anti-mouse CD4 (EPR19514, Abcam) were used for primary staining. The next day, sections were incubated with secondary antibody for 30 min with the addition of 1:50 DAPI after the first half an hour. Alexa Fluor 488 goat anti-rabbit IgG (1:500, Invitrogen) and Alexa Fluor 594 goat anti-rat (1:200, abcam) and Alexa Fluor 488 anti-mouse IgG (1:200, Invitrogen) were used for secondary staining. Each step was followed by 3 times of washing step, 5 min each with TBS at RT. Coverslips were applied to the slides using SlowFade Diamond (ThermoFisher, USA).

Sections were viewed using fluorescence microscope (Olympus, France). For PCNA staining, a minimum of five fields were randomly selected throughout the tumor and images were captured to enumerate the positive-stained cells. Meanwhile for CD3, CD4 and CD8, enumeration was performed for the whole tumor tissue. Positive-stained cells were quantified using ImageJ software (<https://imagej.nih.gov/ij/>).

Flow cytometric analysis

Draining lymph node (dLN) and tumor tissues were harvested at day 10 or day 21 post-inoculation, respectively. To extract cells from dLN, the dLNs were excised and immediately placed in cold RPMI media (Life Technologies). The dLN was minced, filtered through a 40 µm strainers and washed at $300 \times g$ for 5 min.

To extract cells from tumor tissue, the tissue was excised and cut into small fragments (1–4 mm) then incubated for 30 min at 37°C in RPMI media containing 1 ml of tumor digestion medium (10 U/ml of Collagenase I, 400 U/ml of Collagenase IV and 30 U/ml of DNase) (Worthington Biochemical, USA) and 1 ml of Non-Enzymatic Cell Dissociation Buffer (Sigma). The tissue was minced, filtered through a 40 µm strainers and washed at $300 \times g$ for 5 min. In order to remove red blood cells in tumor cell suspension, the pellet was resuspended in 5 ml erythrocyte lysis buffer for 10 min at RT, then the cells were washed again.

For the cell staining for flow cytometry, cell suspensions were resuspended in FACS buffer to achieve $1-2 \times 10^7$ cells/ml and blocked with anti-CD16/32 (BD Bioscience). For intracellular staining, cells were permeabilized and fixed using Intracellular Fixation and Fix &

Perm Cell Fixation and Permeabilization kit (Invitrogen, MD, USA) according to manufacturer's instructions.

Staining was performed by using antibodies against CD11c (clone N418, Biolegend), CD80 (16-10A, Biolegend), CD86 (GL-1, Biolegend), CD45 (30-F11, Biolegend), CD3 (145-2C11, Biolegend), CD8 (53 – 6.7, BD Biosciences), CD4 (GK1.5, Biolegend), CD25 (3C7, Biolegend), CD49b (DX5, Biolegend), CD19 (6D5, Biolegend), and FoxP3 (MF-14, Biolegend). Propidium iodide was added at a final concentration of 1 µg/ml for 5 min prior analysis to discriminate dead cells. The data was acquired by FACSVerse with FACSuite software (BD Biosciences) and analysed using FlowJo software package.

Intratumoral cytokine concentration

Tumor were harvested and homogenized in RIPA buffer containing 1% of protease inhibitor cocktail (Abcam) for every 100 mg of tissue. The homogenates were collected and centrifuged at $14\,000 \times g$ for 10 min at 4°C. Bradford Assay kit (Bio-Rad, US) was used to quantify the total protein concentration in tumor tissue homogenates. Tissue homogenates samples were analyzed to study the concentration of cytokine and chemokine (IL-10, IL-2, TNF- α , IFN- γ and MIP-1a) by using a Milliplex Map Mouse Cytokine/Chemokine Magnetic Bead Panel (MerckMillipore, Germany) using a Luminex technology. The protocol was conducted according to manufacturer's instructions.

Statistical analysis

Comparisons in survival between experimental groups were analyzed using Mantel-Cox analysis. Where appropriate, Mann-Whitey U Test and *t*-test were used to compare median and mean of differences in number of positive cells. ANOVA was used to compare means between groups at different timepoints. Differences were considered significant at *P* value of less than 0.05. All statistical analyses were carried out within GraphPad Prism version 7.0 (GraphPad Software, CA, USA).

Declarations

ACKNOWLEDGEMENTS

This research was funded by the Ministry of Higher Education Malaysia (FRGS grant no: 4F729) and Universiti Teknologi Malaysia (GUP grant no: 15J87). The author would like to thank Universiti Teknologi Malaysia for awarding the Ainuddin Wahid Scholarship.

AUTHOR CONTRIBUTIONS

W.F.A.W.M.Z. and K.J. conceived and designed the experiments. W.F.A.W.M.Z. performed the experiments, collected and analyzed the data. M.H.H. contributed to immunohistochemical analysis methods and reviewed the data and manuscript. M.I.S. contributed to experimental design. K.J. obtained the funding and reviewed the manuscript. W.F.A.W.M.Z. wrote the manuscript.

Competing Interests: The authors declare no competing interests.

References

1. Zagar, T. M. *et al.* Hyperthermia for locally advanced breast cancer. *Int. J. Hyperthermia*. **26**, 618–624 (2010).
2. Gao, S., Zheng, M., Ren, X., Tang, Y. & Liang, X. Local hyperthermia in head and neck cancer: Mechanism, application and advance. *Oncotarget*. **7**, 57367–57378 (2016).
3. Dewhirst, M. W., Vujaskovic, Z., Jones, E. & Thrall, D. Re-setting the biologic rationale for thermal therapy. **21**,779–790(2005).
4. Wu, F. *et al.* 'Wide local ablation' of localized breast cancer using high intensity focused ultrasound. *J Surg Oncol*. **96**, 130–136 (2007).
5. Den Brok, M. H. M. G. M. *et al.* In situ tumor ablation creates an antigen source for the generation of antitumor immunity. *Cancer Res*. **64**, 4024–4029 (2004).
6. Toraya-Brown, S. & Fiering, S. Local tumour hyperthermia as immunotherapy for metastatic cancer. *Int. J. Hyperthermia*. **30**, 531–539 (2014).
7. Tang, F., Zhang, Y., Zhang, J., Guo, J. & Liu, R. Assessment of the efficacy of laser hyperthermia and nanoparticle-enhanced therapies by heat shock protein analysis. *AIP Adv.***4**, (2014).

8. Rao, W., Deng, Z. S. & Liu, J. A review of hyperthermia combined with radiotherapy/chemotherapy on malignant tumors. *Crit. Rev. Biomed. Eng.* **38**, 101–116 (2010).
9. Hegyi, G., Szigeti, G. P. & Szász, A. Hyperthermia versus Oncothermia: Cellular Effects in Complementary Cancer Therapy. *Evid. Based. Complement. Alternat. Med.* 2013, 672873 (2013).
10. Pawlikowska, M., Jędrzejewski, T., Piotrowski, J. & Kozak, W. Fever-range hyperthermia inhibits cells immune response to protein-bound polysaccharides derived from *Coriolus versicolor* extract. *Mol. Immunol.* <https://doi.org/10.1016/j.molimm.2016.10.013> (2016).
11. Happonen, E. *et al.* Thermal dose as a universal tool to evaluate nanoparticle-induced photothermal therapy. *Int. J. Pharm.* **587**, 119657 (2020).
12. Toraya-Brown, S. *et al.* Local hyperthermia treatment of tumors induces CD8 + T cell-mediated resistance against distal and secondary tumors. *Nanomedicine Nanotechnology, Biol. Med.* **10**, 1273–1285 (2014).
13. Pockley, A. G. & Henderson, B. Extracellular cell stress (Heat shock) proteins—immune responses and disease: An overview. *Philos. Trans. R. Soc. B Biol. Sci.* **373**, (2018).
14. Chen, T., Guo, J., Yang, M., Zhu, X. & Cao, X. Chemokine-Containing Exosomes Are Released from Heat-Stressed Tumor Cells via Lipid Raft-Dependent Pathway and Act as Efficient Tumor Vaccine. *J. Immunol.* <https://doi.org/10.4049/jimmunol.1002991> (2011).
15. Zhong, H. *et al.* Induction of a tumour-specific CTL response by exosomes isolated from heat-treated malignant ascites of gastric cancer patients. *Int. J. Hyperth.* <https://doi.org/10.3109/02656736.2011.564598> (2011).
16. Tsang, Y. W. *et al.* Improving immunological tumor microenvironment using electro-hyperthermia followed by dendritic cell immunotherapy. *BMC Cancer.* **15**, 1–11 (2015).
17. Krenacs, T. *et al.* Modulated electro-hyperthermia-induced tumor damage mechanisms revealed in cancer models. *Int. J. Mol. Sci.* <https://doi.org/10.3390/ijms21176270> (2020).
18. I *et al.* Hyperthermia: Cancer Treatment and Beyond. *Intech i*, 13 (2012).
19. Obayashi, T. *et al.* Treatment with near-infrared radiation promotes apoptosis in pancreatic cancer cells. *Oncol. Lett.* **10**, 1836–1840 (2015).
20. Dees, C., Harkins, J., Petersen, M. G., Fisher, W. G. & Wachter, E. A. Treatment of Murine Cutaneous Melanoma with Near Infrared Light. *Photochem. Photobiol.* **75**, 296 (2002).
21. Press, D. Effective near-infrared photodynamic therapy assisted by upconversion nanoparticles conjugated with photosensitizers. 419–432(2015).
22. Guo, L. *et al.* Combinatorial photothermal and immuno cancer therapy using chitosan-coated hollow copper sulfide nanoparticles. *ACS Nano.* **8**, 5670–5681 (2014).
23. Nagaya, T. *et al.* Near infrared photoimmunotherapy targeting EGFR positive triple negative breast cancer: Optimizing the conjugate-light regimen. *PLoS One.* **10**, 1–14 (2015).
24. Strzalka, W. & Ziemienowicz, A. Proliferating cell nuclear antigen (PCNA): A key factor in DNA replication and cell cycle regulation. *Ann. Bot.* **107**, 1127–1140 (2011).
25. Li, J. Y. *et al.* The chemokine receptor CCR4 promotes tumor growth and lung metastasis in breast cancer. *Breast Cancer Res. Treat.* **131**, 837–848 (2012).
26. Mantso, T. *et al.* Hyperthermia induces therapeutic effectiveness and potentiates adjuvant therapy with non-targeted and targeted drugs in an in vitro model of human malignant melanoma. *Sci. Rep.* **8**, 1–16 (2018).
27. Pockley, G. Heat shock proteins as regulators of the immune response. *Lancet.* **362**, 469–476 (2003).
28. Zhou, C. *et al.* Density and location of CD3 + and CD8 + tumor-infiltrating lymphocytes correlate with prognosis of oral squamous cell carcinoma. *J. Oral Pathol. Med.* **47**, 359–367 (2018).
29. Yu, A. *et al.* Presence of lymphocytic infiltrate cytotoxic T lymphocyte CD3+, CD8+, and immunoscore as prognostic marker in patients after radical cystectomy. *PLoS One.* **13**, 1–13 (2018).
30. Gough, M. J. *et al.* OX40 agonist therapy enhances CD8 infiltration and decreases immune suppression in the tumor. *Cancer Res.* **68**, 5206–5215 (2008).

31. Dowling, M. R. *et al.* Regulatory T Cells Suppress Effector T Cell Proliferation by Limiting Division Destiny. *Front. Immunol.* **9**, 2461 (2018).
32. Tang, J. C., Shi, H. S., Wan, L. Q., Wang, Y. S. & Wei, Y. Q. Enhanced Antitumor Effect of Curcumin Liposomes with Local Hyperthermia in the LL / 2 Model. *14*, 2307–2310 (2013).
33. Datta, N. R. *et al.* Local hyperthermia combined with radiotherapy and- / or chemotherapy: Recent advances and promises for the future. *CANCER Treat. Rev.* <https://doi.org/10.1016/j.ctrv.2015.05.009> (2015).
34. Skandalakis, G. P. *et al.* Hyperthermia treatment advances for brain tumors. *Int. J. Hyperth.* **37**, 3–19 (2020).
35. Vargas-roig, L. M., Gago, F. E., Tello, O., Aznar, J. C. & Ciocca, D. R. Heat Shock Protein Expression and Drug Resistance in Breast Cancer Patients Treated with Induction Chemotherapy. *Int. J. Cancer.* [https://doi.org/10.1002/\(SICI\)1097-0215\(19981023\)79](https://doi.org/10.1002/(SICI)1097-0215(19981023)79) (2015).
36. Linthorst, M. *et al.* Local control rate after the combination of re-irradiation and hyperthermia for irresectable recurrent breast cancer: Results in 248 patients. *Radiother. Oncol.* **117**, 217–222 (2015).
37. Datta, N. R., Stutz, E., Gomez, S. & Bodis, S. Efficacy and Safety Evaluation of the Various Therapeutic Options in Locally Advanced Cervix Cancer: A Systematic Review and Network Meta-Analysis of Randomized Clinical Trials. *International Journal of Radiation Oncology Biology Physics.* <https://doi.org/10.1016/j.ijrobp.2018.09.037> (2019).
38. Franckena, M. *et al.* Long-Term Improvement in Treatment Outcome After Radiotherapy and Hyperthermia in Locoregionally Advanced Cervix Cancer: An Update of the Dutch Deep Hyperthermia Trial. *Int. J. Radiat. Oncol. Biol. Phys.* <https://doi.org/10.1016/j.ijrobp.2007.07.2348> (2008).
39. Notter, M., Germond, J. F., Wolf, E., Berz, R. & Berz, J. P. Thermography guided irradiation using water-filtered infrared-A (wIRA) and radiotherapy on recurrent breast cancer - First experiences and temperature analysis. *Thermol. Int.* **21**, 47–53 (2011).
40. Chircop, M. & Speidel, D. Cellular stress responses in cancer and cancer therapy. *Front. Oncol.* **4**, 8–9 (2014).
41. Juríková, M., Danihel, Ä., Polák, Å. & Varga, I. Ki67, PCNA, and MCM proteins: Markers of proliferation in the diagnosis of breast cancer. *Acta Histochem.* <https://doi.org/10.1016/j.acthis.2016.05.002> (2016).
42. Qiu, X. *et al.* Correlation analysis between expression of PCNA, Ki-67 and COX-2 and X-ray features in mammography in breast cancer. *Oncol. Lett.* **14**, 2912–2918 (2017).
43. Zininga, T., Ramatsui, L. & Shonhai, A. Heat shock proteins as immunomodulants. *Molecules***23**, (2018).
44. O'Shea, J. & Paul, W. E. Mechanisms underlying lineage commitment and plasticity of helper CD4 + T cells. *Science.* <https://doi.org/10.1126/science.1178334> (2010).
45. Dobrzanski, M. J. Expanding roles for CD4 T cells and their subpopulations in tumor immunity and therapy. *Frontiers in Oncology.* <https://doi.org/10.3389/fonc.2013.00063> (2013).
46. Terunuma, H. Potentiating immune system by hyperthermia. in *Hyperthermic Oncology from Bench to Bedside* (2016). doi:10.1007/978-981-10-0719-4_12.
47. Mojic, M., Takeda, K. & Hayakawa, Y. The dark side of IFN- γ : Its role in promoting cancer immunoevasion. *Int. J. Mol. Sci.* **19**, 1–13 (2018).
48. Jarnicki, A. G., Lysaght, J., Todryk, S. & Mills, K. H. G. Suppression of Antitumor Immunity by IL-10 and TGF- β -Producing T Cells Infiltrating the Growing Tumor: Influence of Tumor Environment on the Induction of CD4 + and CD8 + Regulatory T Cells. *2–10*(2006).
49. Plitas, G., Rudensky, A. Y. & Regulatory T Cells in Cancer. (2020).
50. Romagnoli, G. *et al.* Morphological evaluation of tumor-infiltrating lymphocytes (TILs) to investigate invasive breast cancer immunogenicity, reveal lymphocytic networks and help relapse prediction: A retrospective study. *Int. J. Mol. Sci.***18**, (2017).
51. Takada, K. *et al.* Use of the tumor-infiltrating CD8 to FOXP3 lymphocyte ratio in predicting treatment responses to combination therapy with pertuzumab, trastuzumab, and docetaxel for advanced HER2-positive breast cancer. *J. Transl. Med.* **16**, 1–11 (2018).
52. Muthana, M., Multhoff, G. & Pockley, A. G. Tumour infiltrating host cells and their significance for hyperthermia. **6736**, (2010).
53. Yagawa, Y., Tanigawa, K., Kobayashi, Y. & Yamamoto, M. Cancer immunity and therapy using hyperthermia with immunotherapy, radiotherapy, chemotherapy, and surgery. *J. Cancer Metastasis Treat.* **3**, 218 (2017).

Figures

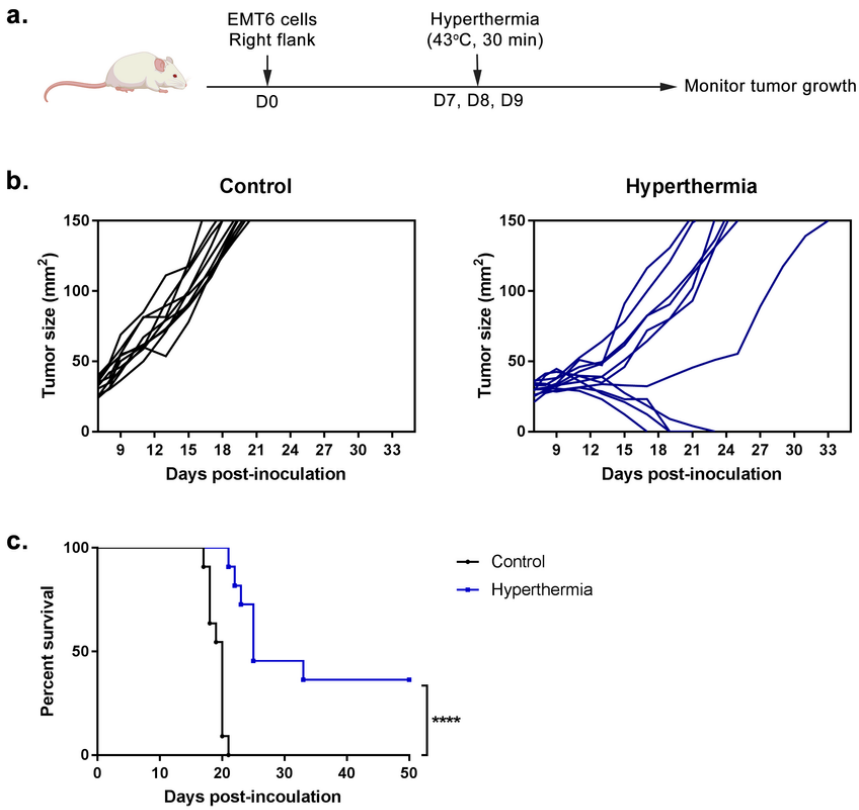


Figure 1

Local hyperthermia by NIR reduces tumor growth in tumor-bearing mice. (a) Schematic time course to study EMT6 tumor progression following treatment. (b) Line graph depicting the individual tumor growth in control and treated group (c) Survival curves of mice in 50 days after treatment. n=11 per group. ****P<0.0001 (Mantel-Cox analysis).

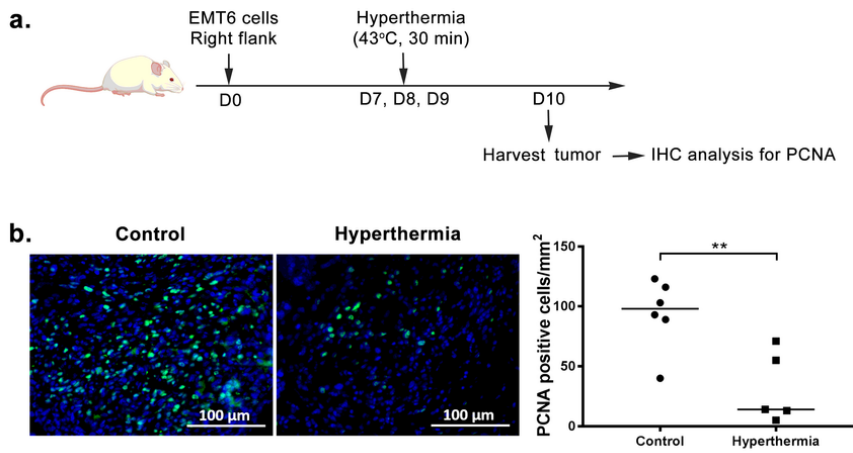


Figure 2

Local hyperthermia by NIR reduces tumor cells proliferation. Mice were sacrificed 3 days after the first treatment. (a) Schematic time course to examine the proliferating cells. (b) Fluorescence macrograph showing the expression of PCNA indicating the proliferating tumor cells and graph showing PCNA positive-stained cells per mm². n=5/6 per group. **P < 0.005 (Student's t-test).

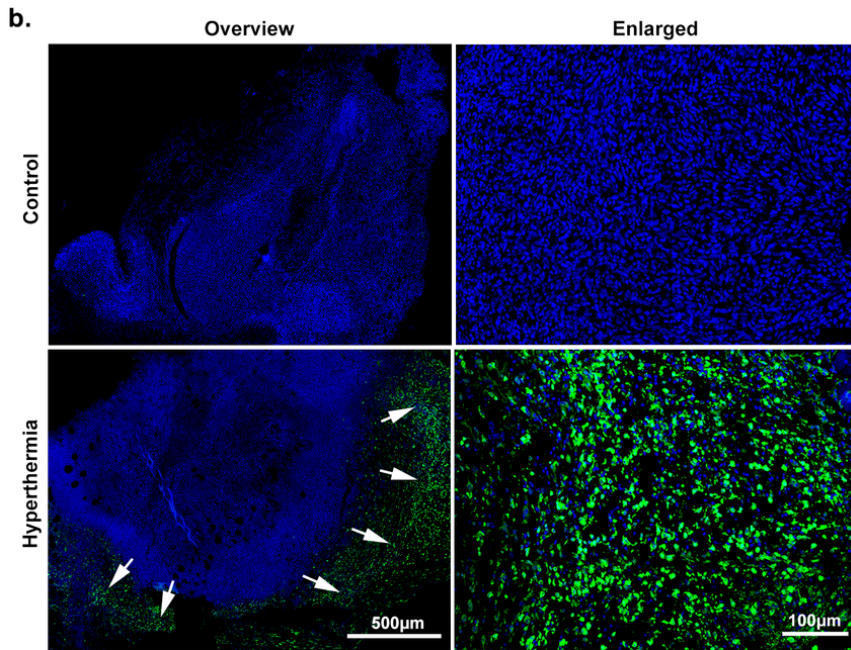
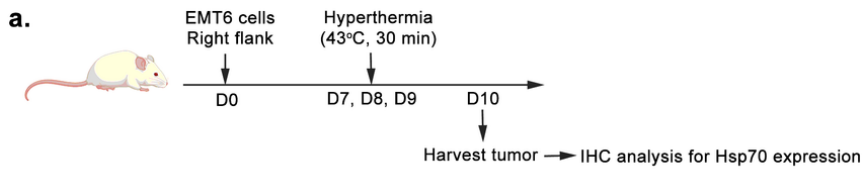


Figure 3

Local hyperthermia by NIR increases tumor Hsp70 expression. Mice were sacrificed 3 days after the first treatment. (a) Schematic time course to measure the Hsp70 expression. (b) Fluorescence micrograph showing the expression of Hsp70 (shown in green) in tumor. Arrow indicates the area of Hsp70 abundance. n=5/6 per group.

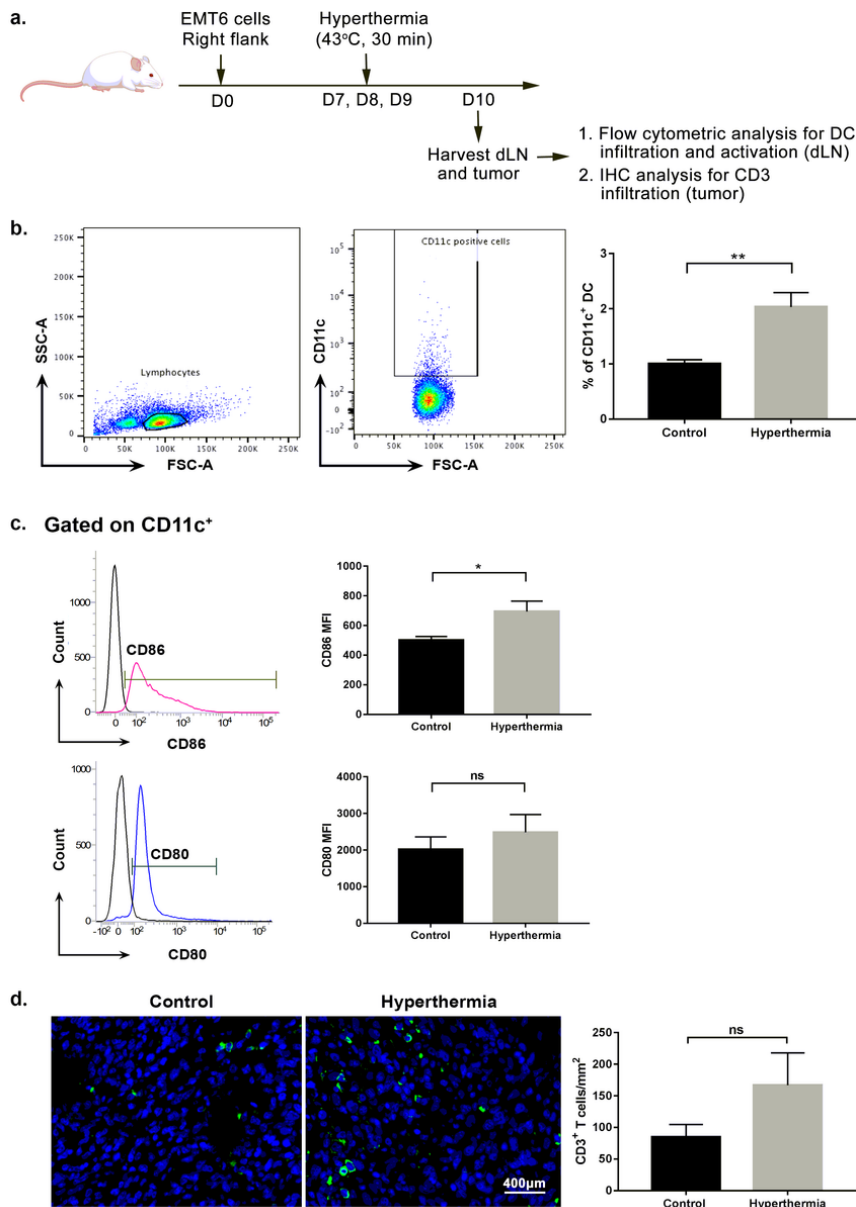


Figure 4

Local hyperthermia by NIR increases DC activation in lymph node and tumor-infiltrated T cells. Mice were sacrificed 3 days after the first treatment. Lymph nodes were analyzed by flow cytometric analysis while tumor was stained for immunohistochemical analysis. (a) Schematic timecourse to measure the activation of DC in dLN and the infiltration of CD3 T cells in tumor. (b) Dot plot showing the gating strategy of CD11c. Cells were gated based on forward and side scatter profile to exclude the doublet cells. Lymphocytes were then gated and further analyzed for the percentage of CD11c as shown in graph. DCs activation increases following hyperthermia treatment, compared to untreated group. (c) Graph showing Mean Fluorescence Intensity (MFI) of CD80 and CD86 expression (\pm mean) on CD11c⁺ cells. (d) CD3 T cell numbers are shown as the median of CD3 cells per mm². Each point represents an individual mouse. n=5/6 per group. ns-P > 0.05, *P < 0.05, **P < 0.005 (Student's t-test).

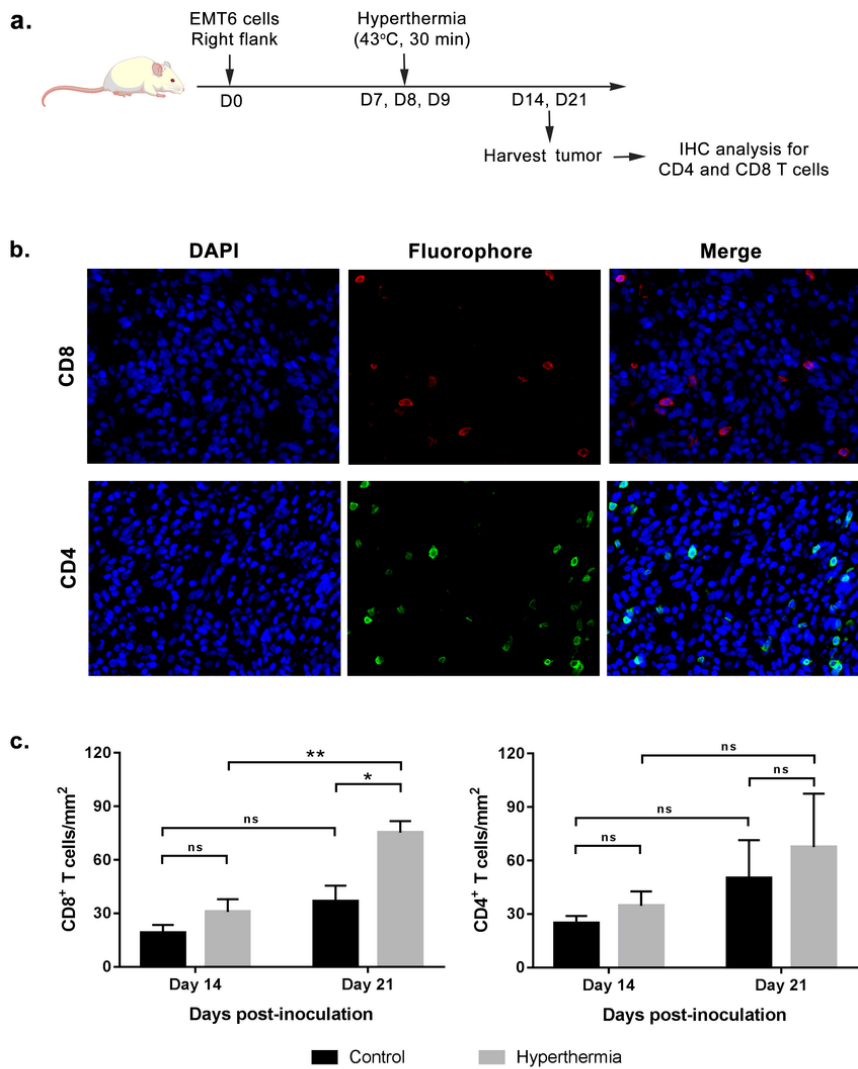


Figure 5

CD8 and CD4 T cells infiltrated in tumor increases over time. Mice were sacrificed at two time points after the treatment; day 14 and day 21 post-inoculation. Tumor were harvested and paraffin-fixed for staining with anti-CD4 and ant-CD8 antibody. (a) Schematic time course to measure the number of tumor-infiltrated CD4+ and CD8+ cells by immunohistochemical analysis. (b) Representative fluorescence images of stained tumor. (c) CD4+ T and CD8+ cell numbers are shown as the median of cells per mm². Each point represents an individual mouse. n=3-6 per group. ns-P > 0.05, *P < 0.05, **P < 0.005 (ANOVA).

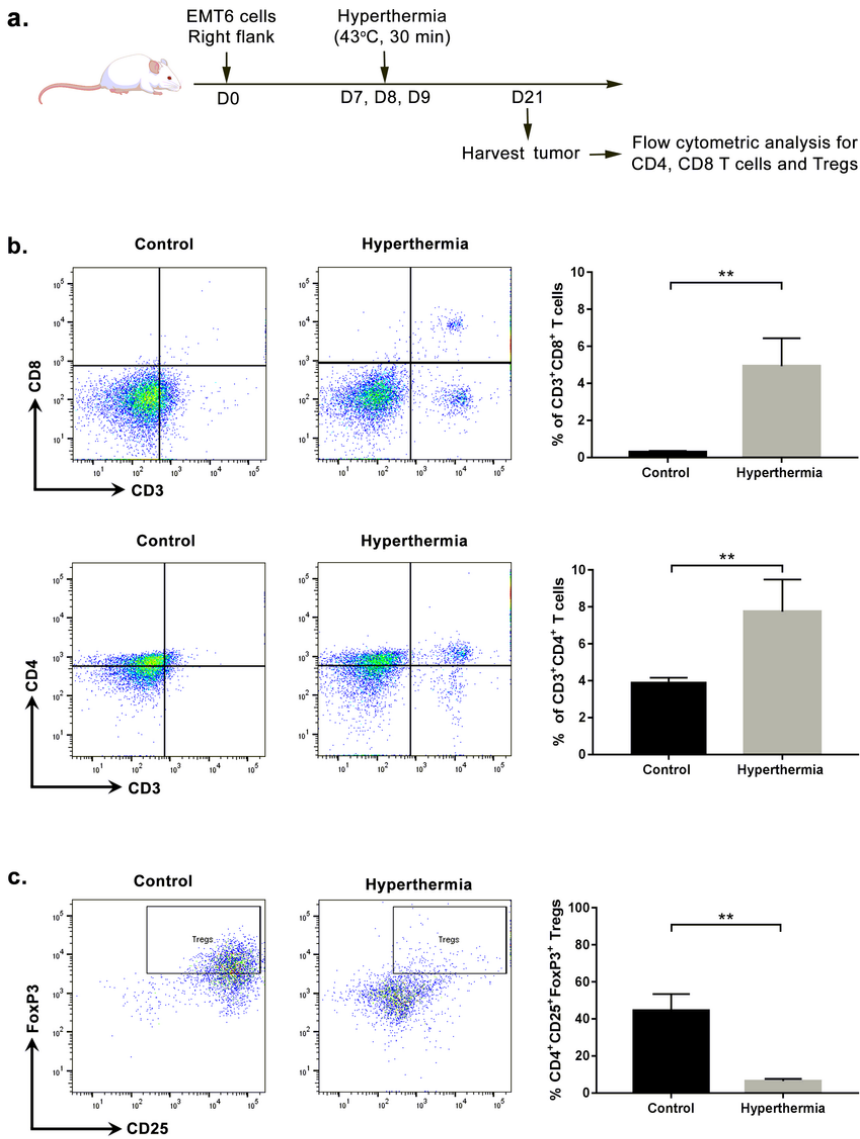


Figure 6

Influence of local hyperthermia by NIR on T cells. Mice were sacrificed 14 days after treatment to evaluate T cells infiltrated at tumor site. Single cells suspension was analyzed by flow cytometric analysis. (a) Schematic timecourse to study the tumor-infiltrated T cells. (b) Representative dot plot showing population of CD4 and CD8 T cells infiltrated in tumor. Graph showing percentage of CD3⁺CD8⁺ and CD3⁺CD4⁺ T cells (\pm mean). (c) Representative dot plot showing population of Tregs infiltrated in tumor. Gated CD4⁺ cells were measured for co-expression of CD25 and FoxP3. Graph showing the percentage of CD4⁺CD25⁺FoxP3⁺ cells (\pm mean). n=5 per group. ns-P > 0.05, **P < 0.005 (Mann-Whitney test).

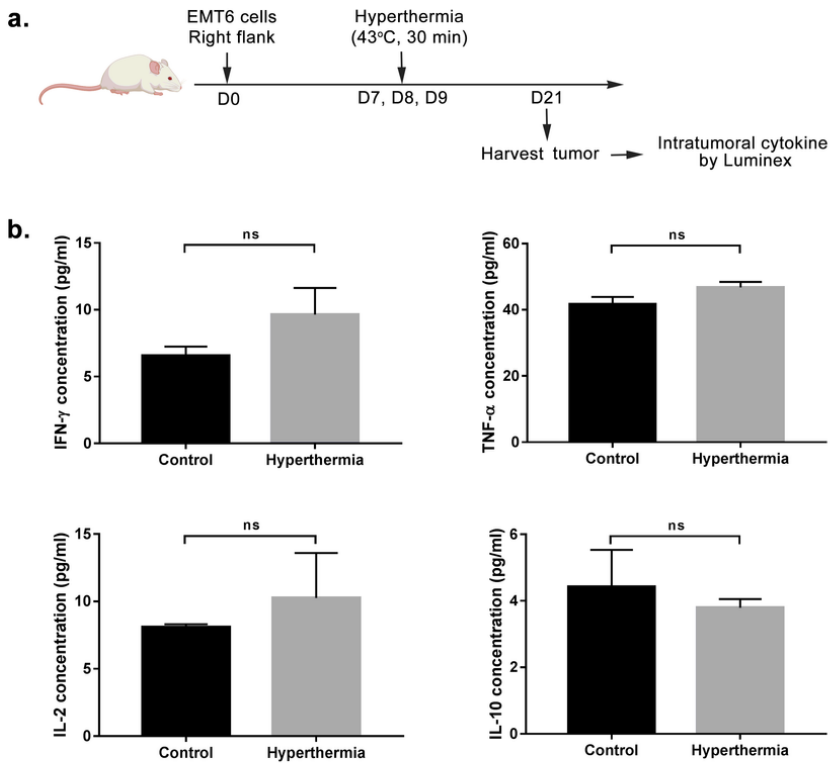


Figure 7

Effect of local HT by NIR on intratumoral cytokine. Mice were sacrificed 2 weeks after the first treatment. Tumor were harvested and total protein concentration were measured. The level of intratumoral cytokine IFN- γ , TNF- α , IL-2, and IL-10 were then analyzed by Luminex. Bar graph showing (a) IFN- γ , (b) TNF- α , (c) IL-2 and (d) IL-10 concentration (\pm mean). n=5/6 per group. ns-P > 0.05 (Student's t-test).

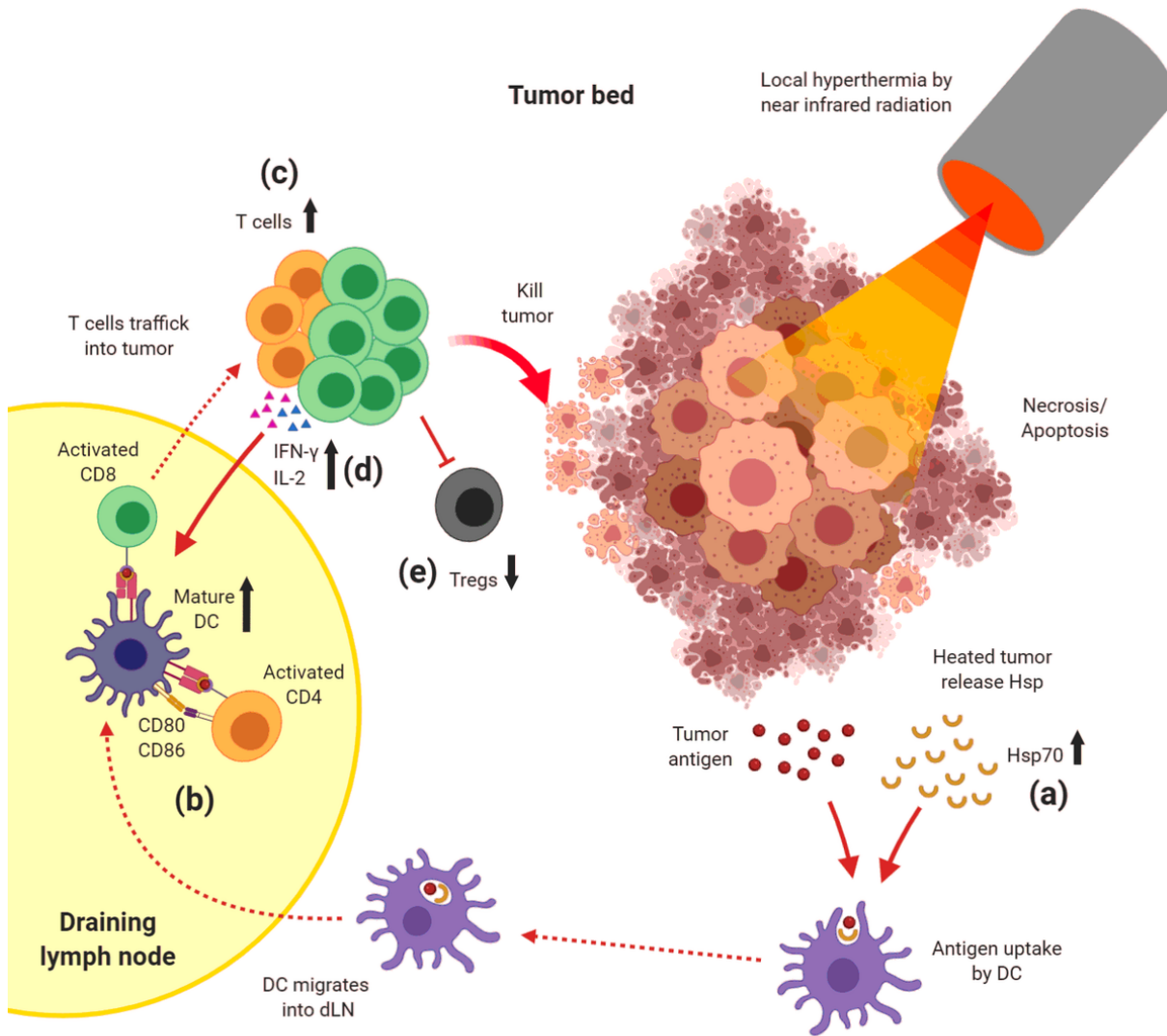


Figure 8

Illustration of anti-tumor immune response induced by monotherapy of local hyperthermia by NIR. NIR induce the released of (a) Hsp from dying cells which increase the activation of (b) CD11c, resulting in the infiltration of (c) T cells into tumor. This is accompanied with the suppression of (d) Tregs infiltrating tumor. NIR also increase (e) IFN- γ and IL-2 secretion in tumor.

Supplementary Files

This is a list of supplementary files associated with this preprint. Click to download.

- [SupplementaryInformationHyperthermiabyNearInfraredRadiationInducedImmuneCellsActivationandInfiltrationinBreastTumor.docx](#)
- [SupplementaryFigure.tif](#)